



The X-linked inhibitor of apoptosis protein (XIAP) is involved in melanoma invasion by regulating cell migration and survival

Ouissam Ayachi¹ · Meltem Barlin¹ · Pia Nora Broxtermann² · Hamid Kashkar² · Cornelia Mauch¹ · Paola Zigrino^{1,3}

Accepted: 4 February 2019 / Published online: 18 February 2019
© International Society for Cellular Oncology 2019

Abstract

Background The X-linked inhibitor of apoptosis (XIAP) is a potent cellular inhibitor of apoptosis, based on its unique capability to bind and to inhibit caspases. However, XIAP is also involved in a number of additional cellular activities independent of its caspase inhibitory function. The aim of this study was to investigate whether modulation of XIAP expression affects apoptosis-independent functions of XIAP in melanoma cells, restores their sensitivity to apoptosis and/or affects their invasive and metastatic capacities.

Methods XIAP protein levels were analyzed by immunohistochemical staining of human tissues and by Western blotting of melanoma cell lysates. The effects of pharmacological inhibition or of XIAP down-regulation were investigated using ex-vivo and transwell invasion assays. The biological effects of XIAP down-regulation on melanoma cells were analyzed in vitro using BrdU/PI, nucleosome quantification, adhesion and migration assays. In addition, new XIAP binding partners were identified by co-immunoprecipitation followed by mass spectrometry.

Results Here we found that the expression of XIAP is increased in metastatic melanomas and in invasive melanoma-derived cell lines. We also found that the bivalent IAP antagonist birinapant significantly reduced the invasive capability of melanoma cells. This reduction could be reproduced by downregulating XIAP in melanoma cells. Furthermore, we found that the migration of melanoma cells and the formation of focal adhesions at cellular borders on fibronectin-coated surfaces were significantly reduced upon XIAP knockdown. This reduction may depend on an altered vimentin-XIAP association, since we identified vimentin as a new binding partner of XIAP. As a corollary of these molecular alterations, we found that XIAP down-regulation in melanoma cells led to a significant decrease in invasion of dermal skin equivalents.

Conclusion From our data we conclude that XIAP acts as a multifunctional pro-metastatic protein in skin melanomas and, as a consequence, that XIAP may serve as a therapeutic target for these melanomas.

Keywords Melanoma · Migration · XIAP · Fibronectin

Ouissam Ayachi and Meltem Barlin equally contributed

Electronic supplementary material The online version of this article (<https://doi.org/10.1007/s13402-019-00427-1>) contains supplementary material, which is available to authorized users.

✉ Paola Zigrino
Paola.Zigrino@uni-koeln.de

¹ Department of Dermatology, University of Cologne, Faculty of Medicine and University Hospital Cologne, Cologne, Germany

² Institute for Medical Microbiology, Immunology and Hygiene (IMMIH), Center for Molecular Medicine Cologne (CMMC), CECAD, University of Cologne, Faculty of Medicine and University Hospital Cologne, Cologne, Germany

³ Department of Dermatology, University of Cologne, Faculty of Medicine and University Hospital Cologne, Kerpener Strasse 62, 50937 Cologne, Germany

1 Introduction

Melanoma is an aggressive type of cancer that arises through the transformation of melanocytes. Once reached the metastatic stage, the prognosis for this type of cancer is poor. In the last years, several therapeutic options have been designed for a more personalized treatment of cancer, including melanoma, but the development of therapy resistance remains an important issue [1]. Resistance to apoptosis has been frequently considered as one of the major drivers of disease progression. Apoptosis is mediated by specific cysteine proteases called caspases. Caspases can be activated mainly via two alternative pathways: the extrinsic pathway that is initiated by cell death receptor ligation and results in activation of the initiator caspase-8 and the intrinsic pathway that is initiated by

permeabilization of the mitochondrial outer membrane, thereby releasing mitochondrial pro-apoptotic factors into the cytosol. This release results in activation of the initiator caspase-9 and inactivation of inhibitors of apoptosis (IAPs), respectively [2]. Whereas anti-apoptotic Bcl2 proteins inhibit mitochondrial membrane permeabilization and the release of pro-apoptotic factors, IAPs interfere with the apoptotic cascade by inhibiting caspase activity [3, 4].

One of the mechanisms underlying resistance to apoptosis in cancer cells is over-expression of one or several IAPs [5]. X-linked IAP (XIAP) represents the only IAP family member that is able to directly bind to initiator and effector caspases (caspase-9 and caspase-3 and -7, respectively) thus inhibiting both the intrinsic and extrinsic apoptotic pathways [6, 7]. Based on its anti-apoptotic activity, XIAP has been investigated in several human cancers [8, 9] and its caspase-binding capacity has been therapeutically targeted using small compound IAP antagonists [10]. The therapeutic application of IAP antagonists (peptidomimetic or not) has, however, changed our view on the role of XIAP antagonization, since it has been found that they mainly interfere with the cytotoxic activity of TNF in tumor cells by inhibiting cIAP1 and cIAP2 (cellular inhibitor of apoptosis 1 and 2) [11–13]. In addition to their direct cytotoxic action towards tumor cells, IAP antagonists have been found to inhibit tumor growth by disrupting the tumor vasculature [14].

In melanoma, XIAP is thought to be involved in metastatic progression, as it has been shown to be significantly over-expressed in metastatic compared to primary melanomas [15, 2]. In addition to caspase inhibitory activities, XIAP has been found to promote the pro-survival/inflammatory NF- κ B signaling pathway either via interaction of its BIR1 domain with TAB/TAK1 [16] or via interaction of its BIR2 domain with RIPK2 [17] and to promote anti-bacterial immunity [18]. Next to the regulation of apoptotic and inflammatory processes, XIAP has been found to be involved in the modulation of other cellular processes as well, such as migration [16–19]. As yet, however, the physiological relevance of these observations has not been shown.

In the present study, we show that the expression of XIAP is increased in patients with metastatic melanoma as well as in several invasive human melanoma-derived cell lines. Using melanoma-derived cell lines with variable but high XIAP expression levels, we found that the bivalent IAP antagonist birinapant affects their invasiveness. This effect could be reproduced through sh-RNA-mediated single XIAP down-regulation in an invasive melanoma-derived cell line, BLM. Furthermore, we show that XIAP may regulate melanoma cell migration on fibronectin by modulating focal adhesion distribution and, likely, interaction with vimentin. Collectively, our data indicate that XIAP may play a role in melanoma cell migration and in processes associated with tumor progression.

2 Materials and methods

2.1 Cells and tissues

Melanoma-derived cell lines were maintained in RPMI-1640 medium containing 10% fetal bovine serum (FBS), 2% L-Glutamine and 100 U/ml Penicillin/Streptomycin and 1% non-essential amino acids. The cell lines were routinely assayed for mycoplasma contamination using PCR (PCR Mycoplasma Kit, Promocell, Heidelberg, Germany). A XIAP down-regulation construct and stable transduced melanoma cell lines were generated as described before [19]. Shortly, a pENTR construct was generated using a pair of oligonucleotides derived from XIAP mRNA (XIAP-RNA3, ID: 2733 from Ambion Europe, Huntingdon, United Kingdom) and includes the unique N-19 target as described in the pSUPER RNAi System Manual. After generating an entry clone, the pLenti6/V5DEST XIAP-RNA3 expression vector was created using LR recombination. Viral particles were produced according to the instructions of the manufacturer (pLenti-Dest Gateway system; Invitrogen, Karlsruhe, Germany). The recombinant lentiviral construct was transduced into cells after which stable cell lines were generated using Blasticidin (Invitrogen) selection.

Colo38 and SKmel28 XIAP knockout cell lines were generated using the CRISPR/Cas method according to the manufacturer instructions (XIAP gRNA, ID: HS0000166277; HS0000166279, Sigma, St. Louis, USA). The respective cells were provided by Hamid Kashkar (University of Cologne).

Transient XIAP down-regulation by siRNA (On-TARGET plus Human XIAP ID:331 SMARTpool siRNA, Dharmacon, Colorado, USA) expression was performed using Lipofectamine RNAi MAX (Invitrogen, California, USA). Cells were seeded (2.5×10^5 cells/well) in 6-well plates and grown for 24 h after which 30 pmol siRNA was added for transfection. After 96 h, the efficiency of silencing was assessed using Western blot analysis. MITF levels were measured to ensure that the cells did not differentiate during the transfection/purification procedure.

Archival paraffin blocks of primary human melanomas and metastases (11 NZN, 14 SSM, 23 NMM and 46 Metastasis) were collected upon informed consent from all the subjects involved. Ethical approval was obtained from the Ethics Committee of the University of Cologne.

2.2 Western blotting and sample preparation

Whole cell lysates were generated using RIPA buffer after which protein concentrations were determined using a BCA protein assay (ThermoFisher, Darmstadt, Germany) according to the manufacturer's instructions. Next, the proteins were subjected to SDS-PAGE and transferred to nitrocellulose membranes. The resulting blots were incubated with primary

antibodies overnight at 4 °C (mouse anti-XIAP 1:500, BD Bioscience, Heidelberg, Germany; mouse anti-actin 1:1000 MPbiomedicals, Eschwege, Germany, used as loading control; and rabbit polyclonal to MITF 1:500, ThermoFisher Scientific, Dreieich, Germany). After washing with PBS + 0,5% Tween, the blots were incubated with a secondary horse-radish-peroxidase (HRP)-conjugated antibody. Protein bands were visualized using an ECL Western blotting detection kit (ThermoFisher) after exposure to X-Ray films.

2.3 Immunoprecipitation and proteomic analysis

Cells were grown on fibronectin (FN), Matrigel-coated or uncoated surfaces to sub-confluence, washed twice with PBS, lysed in RIPA buffer and homogenized overnight at 4 °C. Protein G Sepharose® 4Fast Flow (GE Healthcare) was washed with TBS and incubated with an IgG isotype control or specific antibody (rabbit anti-XIAP, Cell Signaling) overnight at 4 °C. After 24 h, the antibody-coupled beads were washed thrice with TBS, after which the protein bound to beads was collected and frozen until use (pre-clearing). Isotype control-beads were incubated with protein lysates for 2 h at 4 °C, centrifuged and washed thrice with TBS. Cleared supernatants were incubated with beads containing the specific antibody, overnight at 4 °C. The next day, proteins that coprecipitated with the anti-XIAP-beads were washed thrice with TBS and eluted by addition of sample buffer containing β -mercaptoethanol. After heating for 10 min at 95 °C and further incubation with Dithiothreitol (DTT 100 mM, 30 min, 55 °C) chloroacetamide (CAA) was added (30 min, room temperature, dark). Finally, the samples were centrifuged and the collected fractions were analyzed by HPLC-MS at the CECAD facility of the University of Cologne as previously described (15).

2.4 Cell and tissue immunofluorescence staining

40.000 cells were plated on plastic or fibronectin (10 μ g/ml) coated coverslips and incubated in medium without FCS for 24 h. After washing with PBS, the cells were fixed with 1% paraformaldehyde (PFA), permeabilized with 0,05% PBST and incubated with primary antibodies (mouse anti- α -tubulin; Sigma, 1:100; rabbit anti-XIAP; Abcam, 1:100; and mouse anti- α -vinculin; Sigma, 1:400). F-actin filaments were stained with phalloidin-488 (Molecular Probes; ThermoFisher). The nuclei were stained with diamidino-2-phenylindole (DAPI). Immunofluorescence staining images were captured using a BIOREVO BZ-9000 fluorescence microscope (Keyence, Neu-Isenburg, Germany). FA quantification was performed using ImageJ. Tissue immunostaining was performed as previously described [20].

2.5 Invasion assay

This assay was performed as previously described [21]. Briefly, 1×10^4 cells were seeded on top of skin composites that were cultured at the air/liquid interphase for 21 days. The bivalent IAP antagonist birinapant (MedChemExpress; MCE, Germany) was added freshly to the media every two days. Paraffin sections of the cultures were stained with H&E, and the migrated distance of the cells into the underlying tissue was microscopically measured under bright field illumination (Leica DM 4000 B; Leica, Wetzlar, Germany). Images were captured using an imaging system (JVC, KY-F75 U camera; Dikus 4.50, Hilgers, Königswinter, Germany).

Alternatively, in vitro invasion assays were performed using transwells (Millicell Cell Culture Inserts, pore size 8 μ m) coated with Growth Factor Reduced Matrigel (BD Bioscience). Cells (2×10^4) in serum-free medium were seeded in each transwell and invasion was induced by placing fibroblast-conditioned media in the lower compartments. After 24 h, cells in the lower part of the membrane facing the well (invaded) were stained with DAPI (1:1000; 1 h, RT; Sigma-Aldrich) and counted.

2.6 Cell death assay

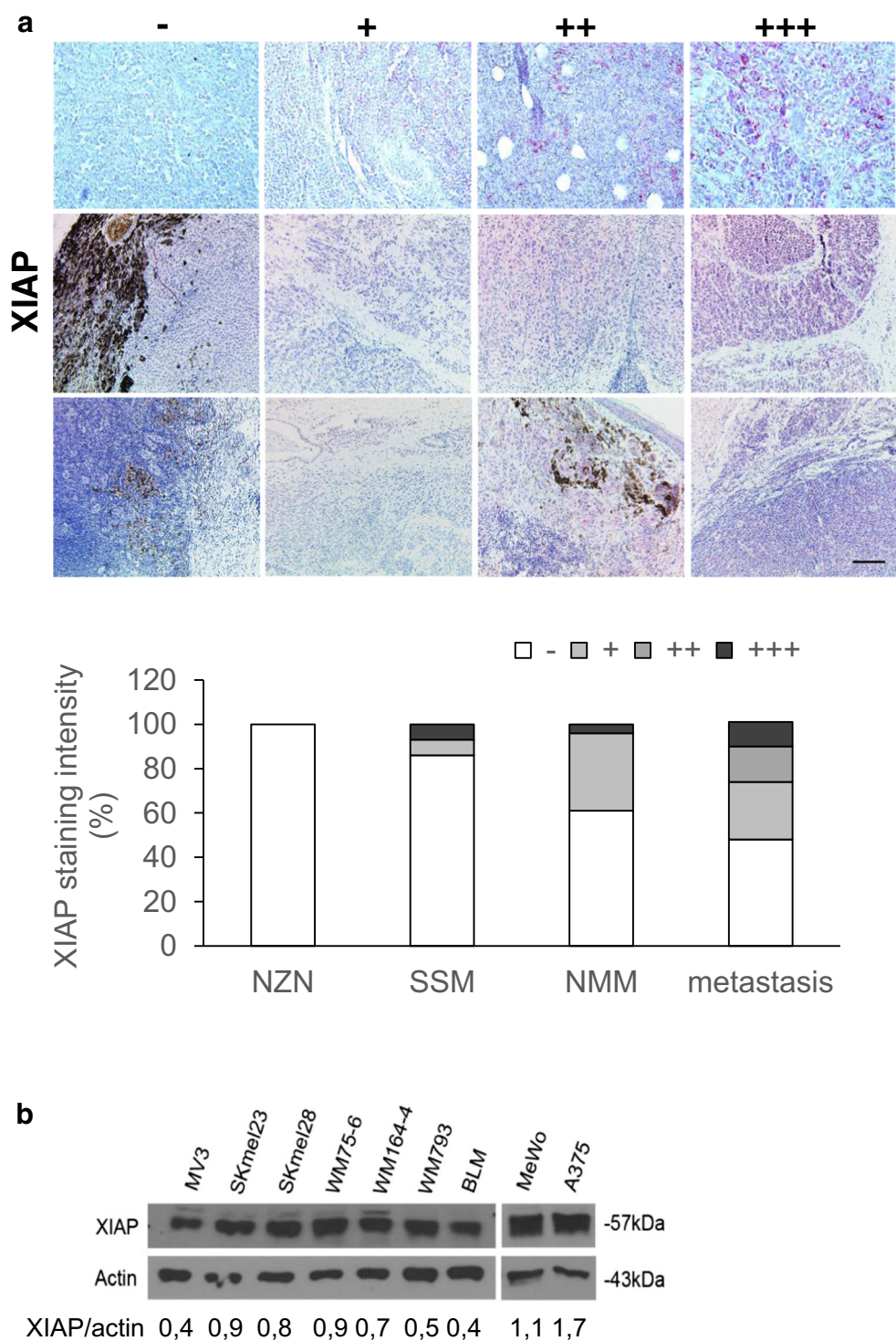
Cells (10^4 per well) were seeded in 96-well plates in medium containing 1% FBS. After 24 h the cells were harvested and cell death was determined using a Cell Death Detection ELISA kit (Roche, Mannheim, Germany).

2.7 Cell adhesion and migration assays

Adhesion assays were performed as described before [22]. Briefly, 96-well tissue culture plates were coated with human plasma fibronectin (10 μ g/ml) overnight at 4 °C. Cells (2×10^4 cells/well) were seeded and incubated in coated/uncoated dishes for 1 h at 37 °C. Adherent cells were stained with 0.5% crystal violet in 20% (v/v) methanol and the optical density (O.D.) of the dye solution was determined at 595 nm.

Cell migration assays were performed in 24-well tissue culture plates as previously described [23]. Cells in monolayer were treated with mitomycin C (1,6 μ g/ml) in serum-free media for 2 h before scratching (scratch wound healing assay) or seeded for colony outgrowth or single cell migration. Only 5–6% of the cells (sh-XIAP and scr control) died upon treatment. For colony outgrowth, 2×10^5 cells were seeded in cloning rings (0.5 mm diameter) placed on uncoated or fibronectin-coated plates and incubated for 2 h at 37 °C. After removing the cloning rings, the plates were placed on a microscope stage heated to 37 °C in a humidified atmosphere after which images were collected every 30 min. Areas covered by cells or migrated distances at the different time points were calculated using Cell[^]R software (Olympus Biosystems, Munich, Germany).

Fig. 1 XIAP expression in human tissues and cells. a Immunohistochemical and Immunohistochemical staining of XIAP in human nevi (NZN), primary melanomas (SSM and NMM) and metastases. Three independent samples are shown for each intensity grade. Samples were scored according to staining intensity as negative (-), low (+), moderate (++) or strong (+++). The graph shows a score plot of XIAP staining for each tissue type. **b** Expression of XIAP in cell lines analyzed by Western blotting. The relative XIAP expression values normalized to actin are shown below



2.8 Statistical analysis

Statistical analyses were performed using Prism GraphPad. Data are expressed as mean ± SD. Comparisons between groups were analyzed using Student’s *t*-tests. *P* values < 0,05 were considered significant.

3 Results

3.1 XIAP expression in primary melanomas and in melanoma-derived cell lines

Previously, XIAP has been found to be significantly over-expressed in metastatic melanomas compared to primary

tumors [15]. Here, we used immunohistochemistry on nevi (NZN), superficial (SSM), nodular (NMM) and metastatic melanoma specimens and assessed XIAP expression intensities at levels arbitrarily set from – to +++ in all tissues (Fig. 1a, right panel). Whereas XIAP was not detected in nevi, it was expressed in primary melanomas and its expression was significantly increased in metastatic melanomas (Fig. 1a). In vitro, variable XIAP expression was detected in the different melanoma-derived cell lines tested (Fig. 1b).

3.2 Therapeutic antagonization of IAPs by birinapant reduces melanoma cell invasiveness

To address the role of XIAP in melanoma invasion, we used three in vivo invasive melanoma cell lines [24–26] that displayed variable XIAP expression levels (A375, BLM, MeWo). The invasive ability of these melanoma cell lines was analyzed using de-epidermized acellular skin onto which cells were seeded and cultured for three weeks. We supplemented the skin composites with the bivalent IAP antagonist birinapant twice a week. After incubation, we calculated the invasive capacity by measuring, in hematoxylin and eosin (H&E) stained sections, the distance by which the cells were migrated into the dermis, expressed as average as reported before [21]. We found that, compared to control composites, birinapant treatment led to a significant reduction in melanoma cell invasion into the dermis in the three melanoma lines tested. The most significant effect was observed for BLM and MeWo cells (Fig. 2).

3.3 Stable down-regulation of XIAP in BLM cells reduces cell invasion

To further address whether XIAP is regulating the invasiveness of metastatic melanoma cells, we down-regulated XIAP expression by stably expressing sh-RNA XIAP mRNA [27]. As a control, cells were transfected with sh-RNA carrying a scrambled sequence (scr), which is not complementary to any human gene. Using real-time PCR analysis, we confirmed a significant reduction (70–95%) in XIAP transcripts in sh-XIAP clones compared to control cells (set as 100%; Supplementary Fig. 1A). This reduction was paralleled by a complete loss of XIAP protein expression in all three clones tested (Supplementary Fig. 1C). In addition, no altered expressions of cIAP1 and -2 were detected in the sh-XIAP clones (Supplementary Fig. 1B). The expression of MITF was not altered by sh-XIAP in BLM cells (Supplementary Fig. 1C) nor in four additional melanoma cell lines in which XIAP expression was efficiently suppressed (Supplementary Fig. 1D), indicating that loss of XIAP expression does not alter the differentiation status of these cells. Notably, we found that sh-XIAP BLM cells displayed an increased susceptibility only when they were exposed to TRAIL, suggesting that the reduced

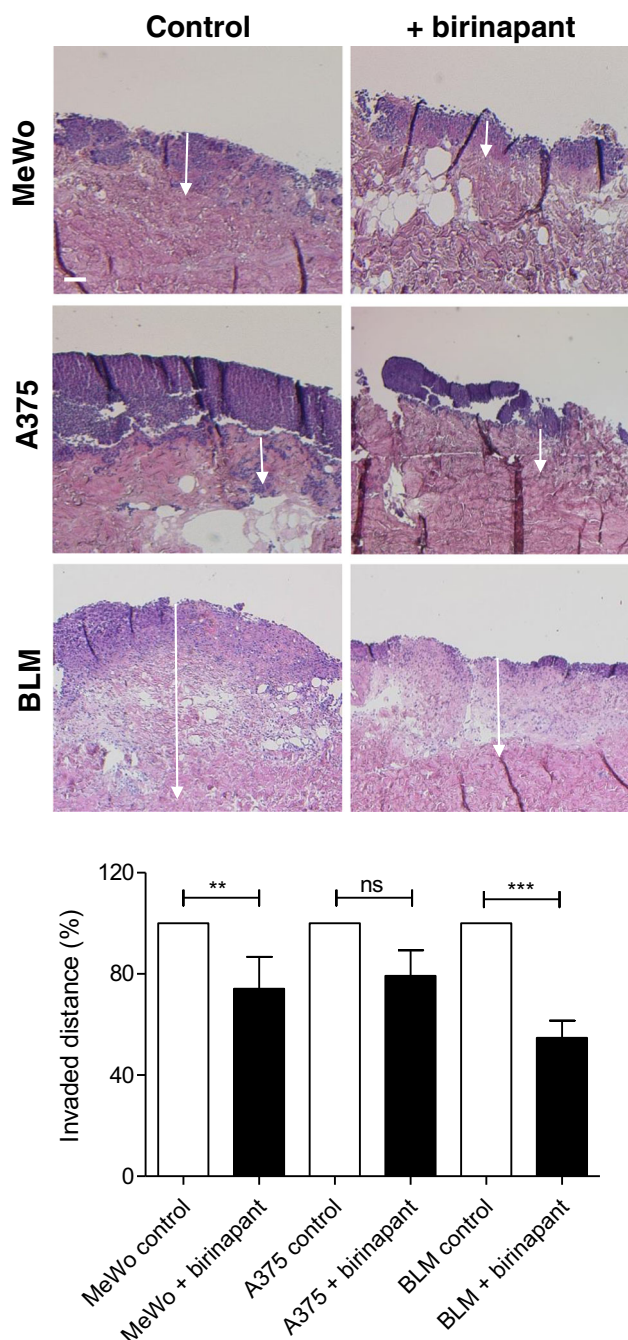


Fig. 2 Dermal invasion of melanoma cells on de-epidermized skin upon treatment with birinapant. Cells were seeded on the dermal side of the acellular dermis and cultured for three weeks with/without mimetics or control compounds. H&E staining of 7 μ m paraffin sections was used to measure the maximal migrated distance of invaded cells (indicated by white arrow). The graph shows the distance invaded by the cells into the dermis (average \pm SD). This experiment was performed in triplicate. ** $p < 0.004$, *** $p < 0.0001$. Scale bar, 100 μ m

migratory activity of cells unlikely results from increased cell death upon XIAP knock-down (Supplementary Fig. 1E).

To address the functional significance for XIAP down-regulation in melanoma cell invasion, we seeded sh-XIAP-BLM cells onto de-epidermized skin and analyzed the ability

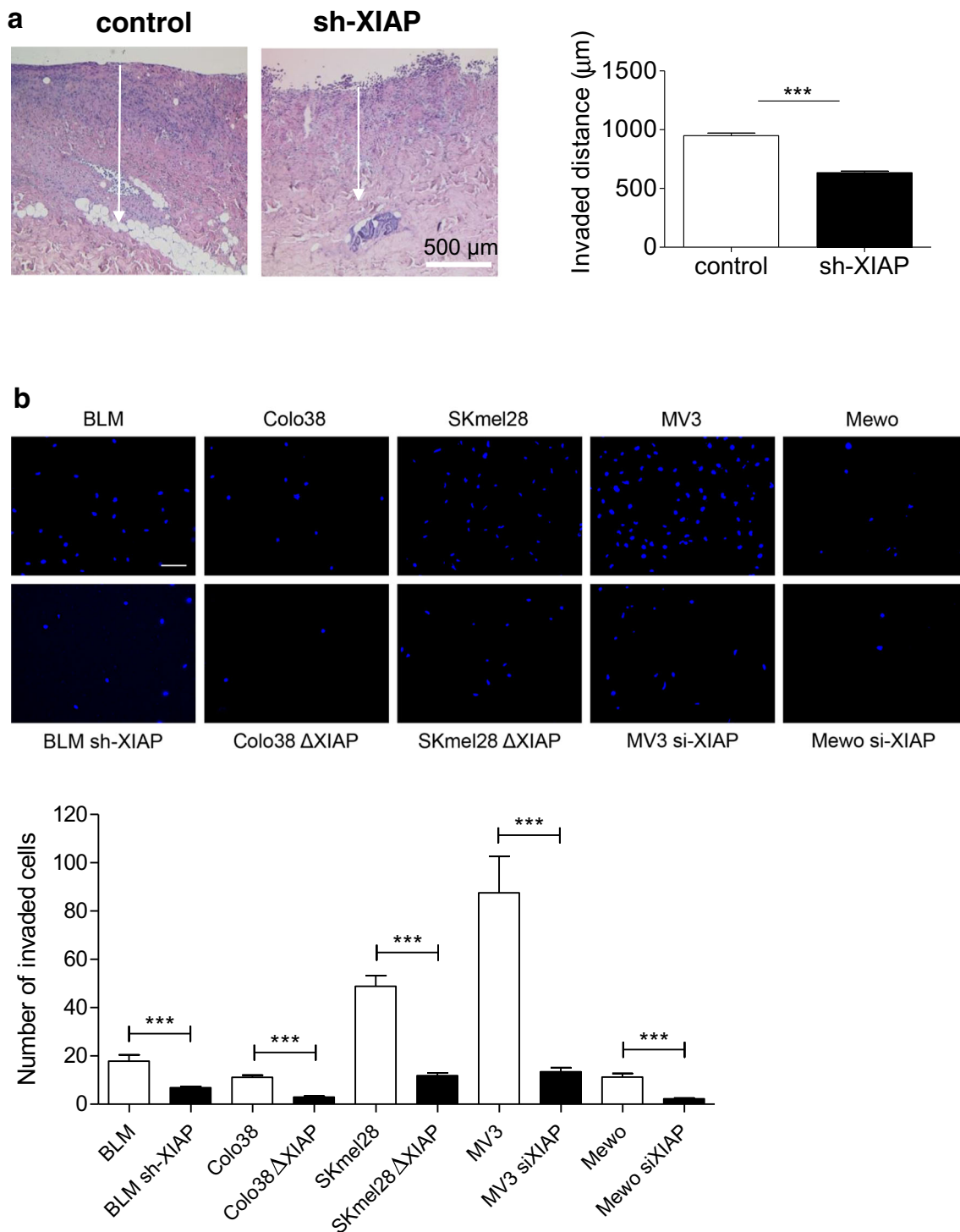


Fig. 3 Invasion of melanoma cells with altered XIAP expression. **a** Control and sh-XIAP clones were seeded on the dermal side of the devitalized dermis. The depth of invaded cells (2 control and sh-XIAP clones each; white arrows) was measured on H&E stained sections. The graph shows quantification of the average migrated distance of control versus sh-XIAP clones \pm SD. **b** Invasion of various melanoma cell lines

(as indicated, with and without XIAP expression; Δ , crisp/cas9 knockout clones; si, transient down-regulation of XIAP using siRNA) through a matrigel on a transwell. The membrane beneath the transwell was stained with DAPI to identify and count the migrated cells (see fluorescence images above; each in triplicate). The number of counted cells is shown as average \pm SD in the graph. *** $p < 0.0001$. Scale bar, 100 μ m

of these cells to penetrate the composites. We found that the average distance by which the cells migrated into the dermis (three clones analyzed, each in quadruplicate) was reduced in

XIAP silenced BLM cells compared to control cells (*** $p < 0.0001$; Fig. 3a). Comparable results were obtained in a transwell-invasion assay using the BLM clones and four

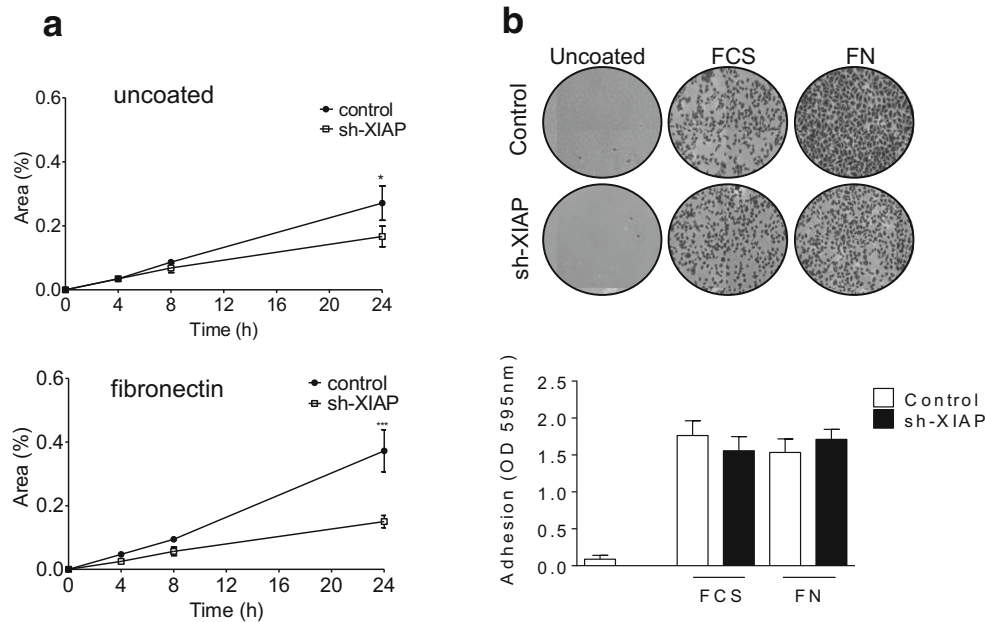


Fig. 4 Adhesion and migration of melanoma cells on fibronectin. **a** Cells were seeded, after mitotic inactivation, into cloning rings on uncoated and fibronectin (10 $\mu\text{g/ml}$) coated plates. After 2 h, rings were removed and unbound cells washed away. Migration of cells was monitored for 24 h and pictures were taken every 30 min. The graphs represent measurements of the gaps at the indicated time points. * $p < 0.05$; *** $p < 0.0001$. **b** To analyze adhesion, a 96-well plate

was coated with 100% FCS and 10 $\mu\text{g/ml}$ fibronectin. After adhesion for 90 min at 37 $^{\circ}\text{C}$, attached cells were stained with 0.5% crystal violet, and the retained dye released by incubation with sodium citrate. Absorbance was measured at 595 nm. Bars (below) represent the mean \pm SD of three experiments carried out in triplicate. Representative photographs are shown of control and sh-XIAP BLM cells adhered to plastic (blocked with BSA), FCS (control) and fibronectin (FN)

additional melanoma cell lines in which the expression of XIAP was suppressed (Fig. 3b). Quantification is shown in a graph (Fig. 3b; below).

3.4 Reduced migration of sh-XIAP-BLM cells

Melanoma cell invasion through the dermis may depend on the ability of the cells to migrate through extracellular matrix networks either as collective sheaths or as single cells [28]. To determine whether XIAP plays a role in collective cell migration we used colony outgrowth assays on plain plastic or fibronectin-coated surfaces. To exclude the influence of cellular proliferation, monolayer cells were pre-treated with mitomycin C before seeding within a cloning ring. After the cells were adhered, cloning rings were removed and outward cell migration was measured over-time by calculating the covered area for up to 24 h. We found that the migration of sh-XIAP BLM clones was reduced after 8 h and was significantly reduced after 24 h on both surfaces (Fig. 4a). Comparable results were obtained using scratch wound and single cell migration assays (Supplementary Fig. 2A and B, respectively). Importantly, we found that the defect observed in cell migration was not due to altered recognition and attachment to the substrate, as cell adhesion to fibronectin was not altered by XIAP knock-down (Fig. 4b).

To test whether depletion of XIAP leads to altered focal adhesion formation and, ultimately, migration defects, we

stained the actin filaments with 488 Φ -phalloidin and subsequently analyzed vinculin localization (in FAs) in cells seeded on fibronectin (FN)-coated surfaces (Fig. 5). We found that the morphology of the cells on FN was not prominently altered, but in sh-XIAP-BLM cells we detected a decreased number of FAs at the cell membrane where bundles of actin filaments converge (Fig. 6; quantification is shown in the lower graphs). The average size of FA in both sh-XIAP and control cells on fibronectin was of 2,5 μm . Within the FA formed in sh-XIAP-BLM cells, we detected significantly reduced numbers of smaller FAs and tendentially increased numbers of larger FAs compared to control cells. Furthermore, we could observe a diffused vinculin staining within the cytoskeleton in the XIAP-deleted BLM cells, suggestive of an altered localization.

3.5 Vimentin associates with XIAP in FN adhered cells

To address the possible proteins associating with XIAP during adhesion to FN, we performed an analysis of proteins that co-immunoprecipitate with XIAP after BLM cell adhesion to FN. We found that a relatively small number of proteins (17) was enriched in the fraction that co-precipitated with XIAP after adhesion to FN compared to adhesion to plastic (volcano plot; Fig. 6). Among these proteins, vimentin, a cytoskeletal protein forming intermediate cytoskeletal filaments, was identified. Using immunofluorescence, we found that vimentin and XIAP closely localized around perinuclear areas rich in

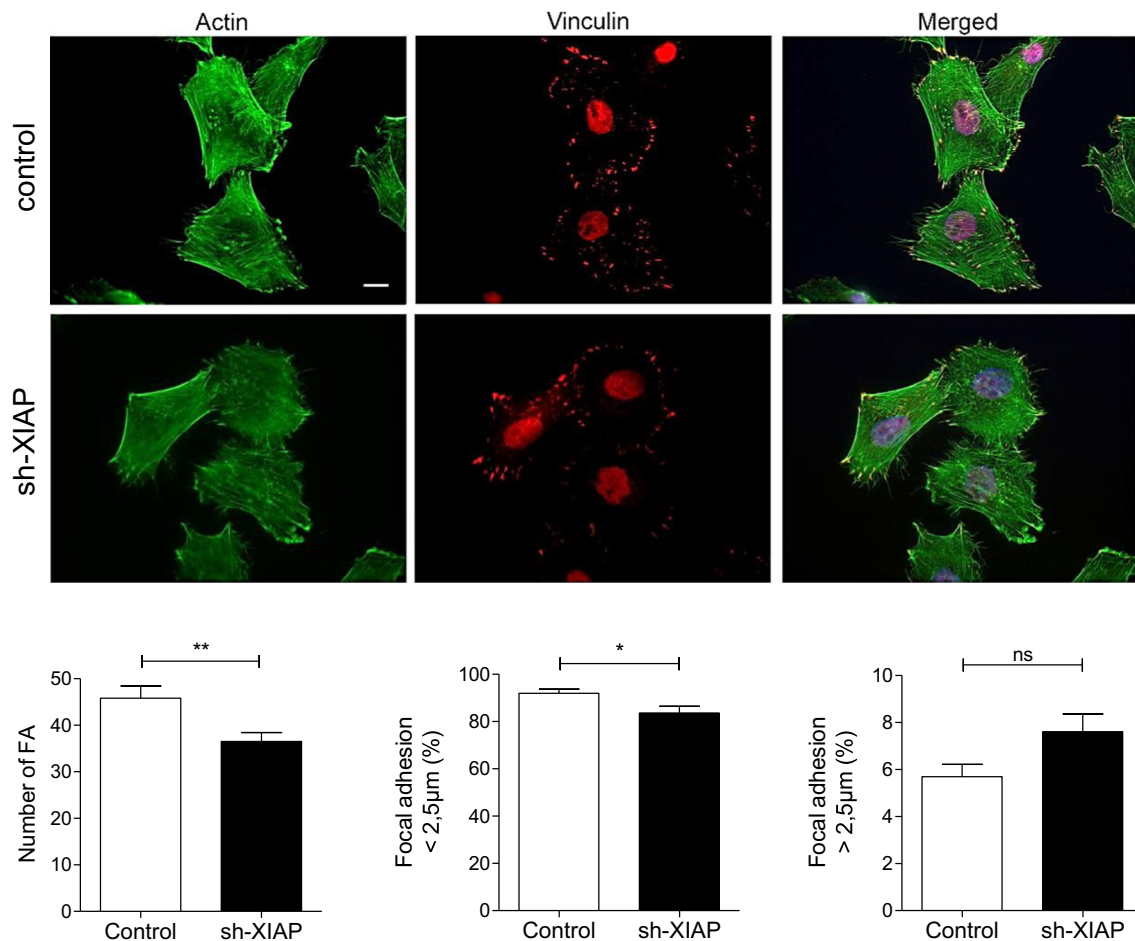


Fig. 5 FA analysis of BLM clones on fibronectin. BLM control cells plated on 10 µg/ml fibronectin for 1 h 40 min were stained for F-actin using phalloidin (green) and for vinculin (red). Nuclei were stained with DAPI (blue). FA numbers and sizes were quantified (below). Averages ±

SD of 64 cells of control (average of two independent control clones) and 105 cells of sh-XIAP clones (average of three sh-XIAP independent clones) are shown. Scale bar, 10 µm

mitochondria in cells plated on plastic (Fig. 7). Upon adhesion to fibronectin, together with the formation of a vimentin network, XIAP was found to diffuse within the cell and to localize at the cell membrane in extensions bound to the substrate (Fig. 7, white arrows). XIAP granules were found to associate along vimentin filaments and both proteins were found to be localized in cell membrane extensions (yellow arrows; and magnifications underneath). Vimentin binding to XIAP was verified through immunoprecipitation of XIAP followed by Western blotting using an anti-vimentin antibody. XIAP precipitation was verified by Western blotting using an anti-XIAP antibody (Fig. 7, right).

4 Discussion

One of the mechanisms underlying apoptosis resistance in tumors involves the regulation of expression of inhibitors such as IAPs [29]. Our data indicate increasing XIAP staining intensities with increasing disease grades, and highest

expression in metastasis suggests that this mechanism may also be active in melanoma. Our data corroborate and complete previously published data [30] and underscore an association with disease progression. Indeed, using an IAP antagonist, we could inhibit ex-vivo invasion of melanoma cells, with a major impact on invasive BLM and MeWo cells. A more variable effect was observed in A375 cells, that have previously been found to be inhibited by non-peptidomimetic IAP compounds [12]. Down-regulation of XIAP could recapitulate this inhibitory effect in BLM cells, using two independent invasion systems. This effect was not limited to BLM cells, as inhibition of XIAP expression in an additional four melanoma-derived cell lines led to impaired invasion in vitro. These data indicate that invasion is primarily modulated by XIAP rather than by other IAPs. Apart from being a regulator of apoptosis, XIAP has been found to exert additional non-apoptotic functions. One important non-apoptotic function of XIAP relevant in the context of tumor cell invasion is the modulation of cell migration. Data obtained from breast and colorectal adenocarcinoma cell lines suggest that

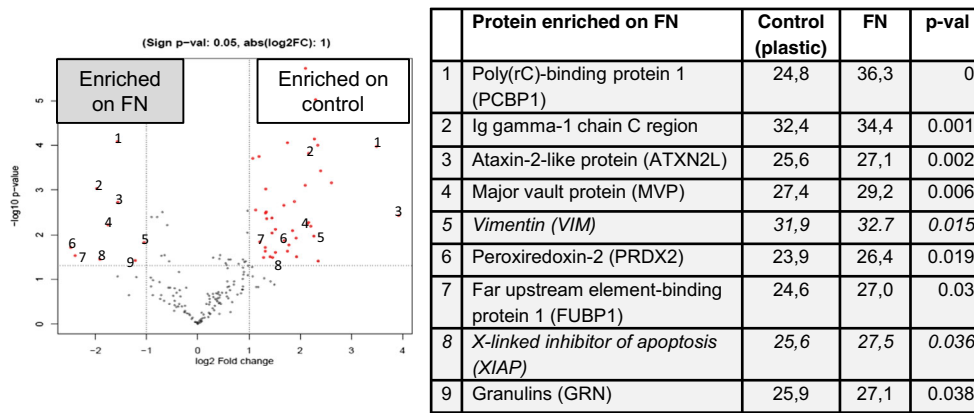


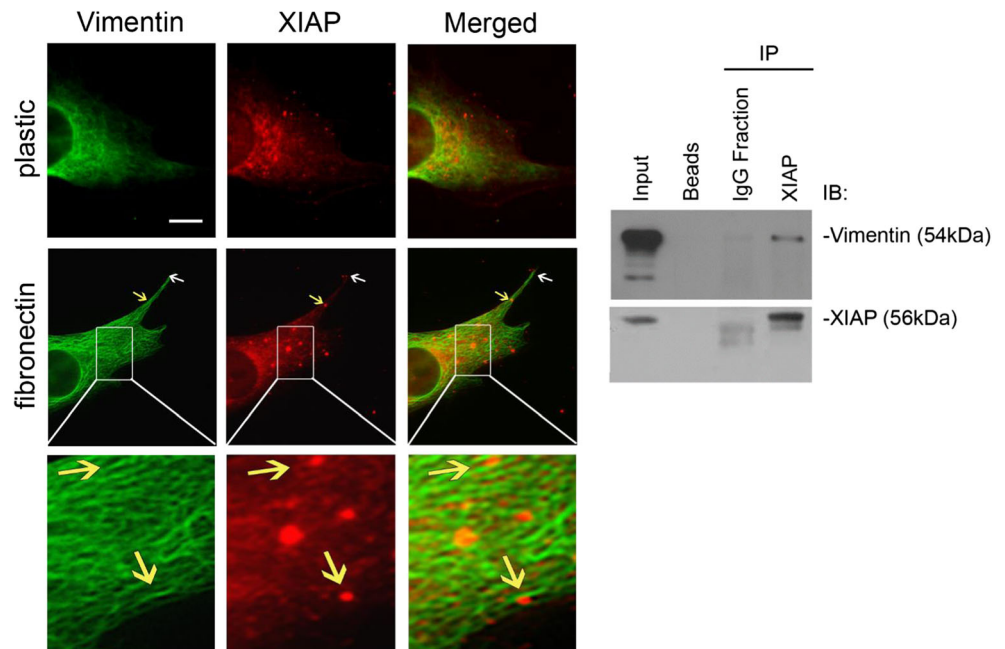
Fig. 6 Proteomic analysis of XIAP co-precipitated proteins upon cell contact with fibronectin. After 24 h of interaction with FN or plastic, the cells were lysed and processed for immunoprecipitation with an anti-XIAP antibody. Co-immunoprecipitated proteins were analyzed by

proteomics. Left, volcano plot displaying enriched protein >1 enriched on FN and <-1 enriched on control expressed as the log10. On the right a table listing all significant proteins co-immunoprecipitated with XIAP

XIAP functions as a direct activator of tumor cell motility and metastasis, independent of its role in cell survival [31]. Our in vitro analyses indicate that the absence of XIAP decreases the single cell and collective migratory abilities of melanoma cells. This effect was observed prominently on fibronectin, present in large amounts in the dermal compartment, and was independent of differences in proliferation and/or cell death rates. This finding is in agreement with previous data [32] showing that direct binding of XIAP to the $\alpha 5$ -integrin/fibronectin complex promotes endothelial cell adhesion and migration. When we performed adhesion assays we were, however, not able to detect any difference in the adhesive ability of XIAP-deficient BLM cells to different substrates compared to that of control cells. This observation suggests that in melanoma cells XIAP is involved in regulating cellular migration

in stages past substrate recognition and adhesion. How at the molecular level XIAP is involved in the regulation of migration is not clearly understood yet, but it may operate in a cell type-specific manner. In colon cancer cells, XIAP deficiency has been found to lead to diminished migration and invasion as a result of reduced β -actin expression and altered cytoskeleton assembly [33]. Murali and colleagues [34] recently showed that down-regulation of XIAP, thus loss of its ubiquitinase function, may lead to enhanced expression and stability of cdc42, a GTPase controlling cell migration. However, in control and sh-XIAP cells plated on fibronectin we barely detected cdc42 expression, indicating that its regulation is not underlying XIAP activity in our cells (data not shown). On the other hand, it has been reported that direct interaction between the RING domain of XIAP and the

Fig. 7 Vimentin-XIAP association. Immunofluorescent analysis showing co-distribution of vimentin and XIAP along filaments (yellow arrows) and at the cell membrane where contact with the matrix takes place (white arrows) in cells cultured on fibronectin for 24 h. A larger magnification of XIAP granules is shown below. Scale bar, 10 μ m. Co-immunoprecipitation of vimentin with XIAP is shown on the right



RhoGDI is necessary for the migration of colon cancer cells [35]. In another study, down-regulation for XIAP or cIAP1 by pharmacological or genetic tools in endometrial and cervical cancer cells resulted in reduced proteasome degradation of Rac1. Elevated Rac1 protein levels and an increase in cell motility was found to be associated with an elongated morphology typical of mesenchymal cells [36]. In sh-XIAP BLM melanoma cells we found that the expression of β -actin and Rac1 and, in addition, RhoA was not changed upon culture on fibronectin (data not shown). Upstream of these GTPases is FAK, and FAK is required for Rho inhibition to promote focal adhesion turnover and cell migration [37]. In a recent study, inhibition of FAK and c-Myc in ovarian cancer cells has been found to lead to disruption of the integrin-FAK axis. In parallel, a decreased expression of XIAP was observed, followed by a reduced cell survival [38]. Whether apart from its involvement in modulating tumor cell survival XIAP may also be involved in the modulation of FAK expression and activity was not considered in this study. Interestingly, we detected fewer FAs formed in sh-XIAP cells adhered to fibronectin, and found that the size distribution was altered compared to that in control cells. The different FA patterns may be responsible for the alterations observed in migration. In fact, Kim and Wirtz [39] have shown that the FA size exhibits a Gaussian relation with cell speed. Thus, either too small or too large, FAs are associated with a reduced migratory velocity, which agrees with our observations and may be causative for the effect observed. XIAP may contribute to FA formation/stabilization by binding to vimentin, as shown by co-immunoprecipitation, in cells plated on fibronectin. Previously, vimentin has been implicated in the modulation of cell migration [40]. Among the activities ascribed to vimentin, it was proposed that recruitment of intermediate filaments to microtubules may induce disassembly of FAs or stabilize them [41]. Vimentin has also been reported to be important in vesicular membrane trafficking, also implicated in controlling adhesive and migratory events (reviewed by [42]). Vimentin can bind integrins, mediate orientation of stress fibers and stabilize FA, ultimately leading to cancer cell migration [43]. Whether XIAP binding to vimentin enhances the activity or stabilizes this protein, ultimately resulting in the regulation of cell migration, remains to be investigated.

Although additional studies are needed to determine the molecules and pathways responsible for XIAP-dependent regulation of cell proliferation and motility in melanoma, we conclude that XIAP contributes to these processes in an apoptosis-independent manner.

Acknowledgments We thank Claudia Coerper-Ochsman for excellent technical assistance. This work was funded by the Deutsche Forschungsgemeinschaft (DFG, German Research Foundation) (grant MA 1181/7-1 to H.K. and C.M.; and Project number 73111208 - SFB 829 (to P.Z. and C.M.).

Compliance with ethical standards

Conflict of interest The authors declare that they have no conflict of interest.

Publisher's note Springer Nature remains neutral with regard to jurisdictional claims in published maps and institutional affiliations.

References

1. E. Shtivelman, M.Q. Davies, P. Hwu, J. Yang, M. Lotem, M. Oren, K.T. Flaherty, D.E. Fisher, Pathways and therapeutic targets in melanoma. *Oncotarget* **5**, 1701–1752 (2014)
2. S. Goldar, M.S. Khaniani, S.M. Derakhshan, B. Baradaran, Molecular mechanisms of apoptosis and roles in cancer development and treatment. *Asian Pac J Cancer Prev* **16**, 2129–2144 (2015)
3. P. Liston, S.S. Young, A.E. Mackenzie, R.G. Korneluk, Life and death decisions: The role of the IAPs in modulating programmed cell death. *Apoptosis* **2**, 423–441 (1997)
4. J. Silke, D. Vucic, IAP family of cell death and signaling regulators. *Methods Enzymol* **545**, 35–65 (2014)
5. S. Fulda, Inhibitor of apoptosis proteins as targets for anticancer therapy. *Expert Rev Anticancer Ther* **7**, 1255–1264 (2007)
6. Y.L. Yang, X.M. Li, The IAP family: Endogenous caspase inhibitors with multiple biological activities. *Cell Res* **10**, 169–177 (2000)
7. B.P. Eckelman, G.S. Salvesen, F.L. Scott, Human inhibitor of apoptosis proteins: Why XIAP is the black sheep of the family. *EMBO Rep* **7**, 988–994 (2006)
8. H. Kashkar, X-linked inhibitor of apoptosis: A chemoresistance factor or a hollow promise. *Clin Cancer Res* **16**, 4496–4502 (2010)
9. Y. Liu, B. Zhang, T. Shi, H. Qin, Inhibition of X-linked inhibitor of apoptosis protein suppresses tumorigenesis and enhances chemosensitivity in anaplastic thyroid carcinoma. *Oncotarget* **8**, 95764–95772 (2017)
10. S. Fulda, Regulation of cell migration, invasion and metastasis by IAP proteins and their antagonists. *Oncogene* **33**, 671–676 (2014)
11. H. Wu, J. Tschopp, S.C. Lin, Smac mimetics and TNF α : A dangerous liaison? *Cell* **131**, 655–658 (2007)
12. G.A. Ward, E.J. Lewis, J.S. Ahn, C.N. Johnson, J.F. Lyons, V. Martins, J.M. Munck, S.J. Rich, T. Smyth, N.T. Thompson, P.A. Williams, N.E. Wilsher, N.G. Wallis, G. Chessari, ASTX660, a novel non-peptidomimetic antagonist of cIAP1/2 and XIAP, potently induces TNF α -dependent apoptosis in Cancer cell lines and inhibits tumor growth. *Mol Cancer Ther* **17**, 1381–1391 (2018)
13. K.S. Prabhu, I.W. Achkar, S. Kuttikrishnan, S. Akhtar, A.Q. Khan, K.S. Siveen, S. Uddin, Embelin: A benzoquinone possesses therapeutic potential for the treatment of human cancer. *Future Med Chem* **10**, 961–976 (2018)
14. A. Witt, J.M. Seeger, O. Coutelle, P. Zigrino, P. Broxtermann, M. Andree, K. Brinkmann, C. Jungst, A.C. Schauss, S. Schull, D. Wohlleber, P.A. Knolle, M. Kronke, C. Mauch, H. Kashkar, IAP antagonization promotes inflammatory destruction of vascular endothelium. *EMBO Rep* **16**, 719–727 (2015)
15. K.D. Bromberg, H.M. Kluger, A. Delaunay, S. Abbas, K.A. DiVito, S. Krajewski, Z. Ronai, Increased expression of the E3 ubiquitin ligase RNF5 is associated with decreased survival in breast cancer. *Cancer Res* **67**, 8172–8179 (2007)
16. M. Lu, S.C. Lin, Y. Huang, Y.J. Kang, R. Rich, Y.C. Lo, D. Myszk, J. Han, H. Wu, XIAP induces NF-kappaB activation via the BIR1/TAB1 interaction and BIR1 dimerization. *Mol Cell* **26**, 689–702 (2007)

17. A. Krieg, R.G. Correa, J.B. Garrison, G. Le Negrate, K. Welsh, Z. Huang, W.T. Knoefel, J.C. Reed, XIAP mediates NOD signaling via interaction with RIP2. *Proc Natl Acad Sci U S A* **106**, 14524–14529 (2009)
18. M. Andree, J.M. Seeger, S. Schull, O. Coutelle, D. Wagner-Stippich, K. Wiegmann, C.M. Wunderlich, K. Brinkmann, P. Broxtermann, A. Witt, M. Fritsch, P. Martinelli, H. Bielig, T. Lamkemeyer, E.I. Rugarli, T. Kaufmann, A. Sterner-Kock, F.T. Wunderlich, A. Villunger, L.M. Martins, M. Kronke, T.A. Kufer, O. Utermohlen, H. Kashkar, BID-dependent release of mitochondrial SMAC dampens XIAP-mediated immunity against *Shigella*. *EMBO J* **33**, 2171–2187 (2014)
19. H. Kashkar, J.M. Seeger, A. Hombach, A. Deggerich, B. Yazdanpanah, O. Utermohlen, G. Heimlich, H. Abken, M. Kronke, XIAP targeting sensitizes Hodgkin lymphoma cells for cytolytic T-cell attack. *Blood* **108**, 3434–3440 (2006)
20. H. Kashkar, C. Haefs, H. Shin, S.J. Hamilton-Dutoit, G.S. Salvesen, M. Kronke, J.M. Jurgensmeier, XIAP-mediated caspase inhibition in Hodgkin's lymphoma-derived B cells. *J Exp Med* **198**, 341–347 (2003)
21. R. Denhofer, P. Kurschat, P. Zigrino, A. Klose, A. Bosserhoff, G. van Muijen, T. Krieg, C. Mauch, N. Hunzelmann, Invasion of melanoma cells into dermal connective tissue in vitro: Evidence for an important role of cysteine proteases. *Int J Cancer* **106**, 316–323 (2003)
22. P. Zigrino, A.S. Kamiguti, J. Eble, C. Drescher, R. Nischt, J.W. Fox, C. Mauch, The repolysin jararhagin, a snake venom metalloproteinase, functions as a fibrillar collagen agonist involved in fibroblast cell adhesion and signaling. *J Biol Chem* **277**, 40528–40535 (2002)
23. C. Mauch, J. Zamek, A.N. Abety, G. Grimberg, J.W. Fox, P. Zigrino, Accelerated wound repair in ADAM-9 knockout animals. *J Invest Dermatol* **130**, 2120–2130 (2010)
24. U.B. Hofmann, J.R. Westphal, E.T. Waas, A.J. Zendman, I.M. Cornelissen, D.J. Ruiters, G.N. van Muijen, Matrix metalloproteinases in human melanoma cell lines and xenografts: Increased expression of activated matrix metalloproteinase-2 (MMP-2) correlates with melanoma progression. *Br J Cancer* **81**, 774–782 (1999)
25. J.M. Kozlowski, I.R. Hart, I.J. Fidler, N. Hanna, A human melanoma line heterogeneous with respect to metastatic capacity in athymic nude mice. *J Natl Cancer Inst* **72**, 913–917 (1984)
26. R.S. Kerbel, M.S. Man, D. Dexter, A model of human cancer metastasis: Extensive spontaneous and artificial metastasis of a human pigmented melanoma and derived variant sublines in nude mice. *J Natl Cancer Inst* **72**, 93–108 (1984)
27. J.M. Seeger, K. Brinkmann, B. Yazdanpanah, D. Haubert, C. Pongratz, O. Coutelle, M. Kronke, H. Kashkar, Elevated XIAP expression alone does not confer chemoresistance. *Br J Cancer* **102**, 1717–1723 (2010)
28. Y. Hegerfeldt, M. Tusch, E.B. Brocker, P. Friedl, Collective cell movement in primary melanoma explants: Plasticity of cell-cell interaction, beta1-integrin function, and migration strategies. *Cancer Res* **62**, 2125–2130 (2002)
29. S. Fulda, D. Vucic, Targeting IAP proteins for therapeutic intervention in cancer. *Nat Rev Drug Discov* **11**, 109–124 (2012)
30. E.L. Hiscott, D.S. Hill, S. Martin, R. Kerr, A. Harbottle, M. Birch-Machin, C.P. Redfern, S. Fulda, J.L. Armstrong, P.E. Lovat, Targeting X-linked inhibitor of apoptosis protein to increase the efficacy of endoplasmic reticulum stress-induced apoptosis for melanoma therapy. *J Invest Dermatol* **130**, 2250–2258 (2010)
31. S. Mehrotra, L.R. Languino, C.M. Raskett, A.M. Mercurio, T. Dohi, D.C. Altieri, IAP regulation of metastasis. *Cancer Cell* **17**, 53–64 (2010)
32. J. Kim, S. Ahn, Y.G. Ko, Y.C. Boo, S.G. Chi, C.W. Ni, Y.M. Go, H. Jo, H. Park, X-linked inhibitor of apoptosis protein controls alpha5-integrin-mediated cell adhesion and migration. *Am J Physiol Heart Circ Physiol* **299**, H300–H309 (2010)
33. J. Liu, D. Zhang, W. Luo, Y. Yu, J. Yu, J. Li, X. Zhang, B. Zhang, J. Chen, X.R. Wu, G. Rosas-Acosta, C. Huang, X-linked inhibitor of apoptosis protein (XIAP) mediates cancer cell motility via rho GDP dissociation inhibitor (RhoGDI)-dependent regulation of the cytoskeleton. *J Biol Chem* **286**, 15630–15640 (2011)
34. A. Murali, J. Shin, H. Yurugi, A. Krishnan, M. Akutsu, A. Carpy, B. Macek, K. Rajalingam, Ubiquitin-dependent regulation of Cdc42 by XIAP. *Cell Death Dis* **8**, e2900 (2017)
35. J. Liu, D. Zhang, W. Luo, J. Yu, J. Li, Y. Yu, X. Zhang, J. Chen, X.R. Wu, C. Huang, E3 ligase activity of XIAP RING domain is required for XIAP-mediated cancer cell migration, but not for its RhoGDI binding activity. *PLoS One* **7**, e35682 (2012)
36. T.K. Oberoi, T. Dogan, J.C. Hocking, R.P. Scholz, J. Mooz, C.L. Anderson, C. Karreman, D. Meyer zu Heringdorf, G. Schmidt, M. Ruonala, K. Namikawa, G.S. Harms, A. Carpy, B. Macek, R.W. Koster, K. Rajalingam, IAPs regulate the plasticity of cell migration by directly targeting Rac1 for degradation. *EMBO J* **31**, 14–28 (2012)
37. X.D. Ren, W.B. Kiosses, D.J. Sieg, C.A. Otey, D.D. Schlaepfer, M.A. Schwartz, Focal adhesion kinase suppresses rho activity to promote focal adhesion turnover. *J Cell Sci* **113**(Pt 20), 3673–3678 (2000)
38. B. Xu, J. Lefringhouse, Z. Liu, D. West, L.A. Baldwin, C. Ou, L. Chen, D. Napier, L. Chaiswing, L.D. Brewer, D. St Clair, O. Thibault, J.R. van Nagell, B.P. Zhou, R. Drapkin, J.A. Huang, M.L. Lu, F.R. Ueland, X.H. Yang, Inhibition of the integrin/FAK signaling axis and c-Myc synergistically disrupts ovarian cancer malignancy. *Oncogenesis* **6**, e295 (2017)
39. D.H. Kim, D. Wirtz, Focal adhesion size uniquely predicts cell migration. *FASEB J* **27**, 1351–1361 (2013)
40. B.M. Chung, J.D. Rotty, P.A. Coulombe, Networking galore: Intermediate filaments and cell migration. *Curr Opin Cell Biol* **25**, 600–612 (2013)
41. R. Bhattacharya, A.M. Gonzalez, P.J. Debiase, H.E. Trejo, R.D. Goldman, F.W. Flitney, J.C. Jones, Recruitment of vimentin to the cell surface by beta3 integrin and plectin mediates adhesion strength. *J Cell Sci* **122**, 1390–1400 (2009)
42. J. Ivaska, H.M. Pallari, J. Nevo, J.E. Eriksson, Novel functions of vimentin in cell adhesion, migration, and signaling. *Exp Cell Res* **313**, 2050–2062 (2007)
43. C.Y. Liu, H.H. Lin, M.J. Tang, Y.K. Wang, Vimentin contributes to epithelial-mesenchymal transition cancer cell mechanics by mediating cytoskeletal organization and focal adhesion maturation. *Oncotarget* **6**, 15966–15983 (2015)